Original Article

Measurement of lysine-specific demethylase-1 activity in the nuclear extracts by flow-injection based time-of-flight mass spectrometry

Chiharu Sakane,[1] Hiromichi Ohta[2] and Yoshihiro Shidoji[1,*]

[1]Molecular and Cellular Biology, Graduate School of Human Health Science, University of Nagasaki, 1-1-1 Manabino, Nagayo, Nishisonogi-gun, Nagasaki 851-2195, Japan
[2]University of Nagasaki, 123 Kawashimo, Sasebo, Nagasaki 858-8580, Japan

(Received 18 August, 2014; Accepted 6 October, 2014; Published online 13 February, 2015)

Lysine-specific demethylase 1 (LSD1/KDM1A), a histone-modifying enzyme, is upregulated in many cancers, especially in neuroblastoma, breast cancer and hepatoma. We have established a simple method to measure LSD1 activity using a synthetic *N*-terminal 21-mer peptide of histone H3, which is dimethylated at Lys-4 (H3K4me2). After the enzyme reaction, a substrate of H3K4me2 and two demethylated products, H3K4me1 and H3K4me0, were quantitatively determined by flow injection time-of-flight mass spectrometry (FI-TOF/MS). By using recombinant human LSD1, a nonlinear fitting simulation of the data obtained by FI-TOF/MS produced typical consecutive-reaction kinetics. Apparent K_m and k_{cat} values of hLSD1 for the first and second demethylation reactions were found to be in the range of reported values. Tranylcypromine was shown to inhibit LSD1 activity with an IC_{50} of 6.9 μM for the first demethylation reaction and 5.8 μM for the second demethylation reaction. The FI-TOF/MS assay revealed that the endogenous LSD1 activity was higher in the nuclear extracts of SH-SY5Y cells than in HeLa or PC-3 cells, and this is in accordance with the immunoblotting data using an anti-LSD1 antibody. A simple, straightforward FI-TOF/MS assay is described to efficiently measure LSD1 activity in the nuclear extracts of cultured cells.

***Key Words*:** **lysine-specific demethylase 1, time-of-flight mass spectrometry, consecutive reactions, epigenetics**

Epigenetic mechanisms are essential for development and differentiation in mammals and epigenetic alterations are key features of cancer, leading to aberrant gene functions.[1,2] Epigenetic changes in cancers cause a global hypomethylation of genomic DNA that result in genomic instability and activation of growth-promoting genes. Such changes also lead to site-specific hypermethylation of the promoter region CpG islands, which results in silencing tumor-suppressor genes, and a global loss of acetylated histones caused by histone deacetylases. This global loss triggers nucleosome remodeling.

In addition to histone acetylation, lysine methylation of histones is also heavily involved in nucleosome remodeling and gene expression. The methylation status is reversibly regulated by histone lysine methyltransferases and histone lysine demethylases (KDMs). Although a number of KDMs have been identified, lysine-specific demethylase 1 (LSD1, also known as KDM1A, BHC110 or AOF2) has recently received noticeable attention following its identification in 2004.[3] LSD1 is capable of removing dimethyl and monomethyl groups on lysine-4 of histone H3, as well as methyl groups of non-histone proteins such as the tumor suppressor p53 and DNA-methyltransferase 1.[4] LSD1 is a member of the flavin-dependent amine oxidase (AOF) superfamily, and is similar in 3D structure to monoamine oxidases A and B, and polyamine oxidase.[4,5] Therefore, tranylcypromine or *trans*-2-phenylcyclopropylamine (2-PCPA), a pan inhibitor against amine oxidases, is also able to act as a suicide substrate of LSD1 by covalently linking to FAD on the enzyme.[5,6] LSD2, also known as KDM1B or AOF1, is the only other paralogue of the LSD1 in AOF family and shows the same substrate specificity.[7] LSD2 is rich in oocytes and is thought to participate in genomic imprinting.[8]

Overexpression of LSD1 is frequently observed in prostate, breast and bladder cancers, and especially neuroblastoma, where overexpression correlates directly with adverse outcomes and inversely with differentiation in neuroblastic tumors.[9] Thus, LSD inhibitors are potential anticancer agents that may be suitable for application in other human diseases that exhibit mis-regulation of gene expression. For example, 2-PCPA has been shown to induce differentiation of acute myelocytic leukemia with combinatorial use of all-*trans* retinoic acid[10] and single-handedly suppressed growth of several neuroblastoma cell lines *in vitro*, as well as neuroblastoma xenograft growth *in vivo*.[7] LSD1 currently represents an emerging epigenetic target class for the discovery of novel anti-tumor therapies.[2]

By scrutinizing a putative pivotal role of LSD1 in epigenetic regulation of carcinogenesis, it is fundamentally important to assess not only the amount of the protein, but also the enzyme activity in samples. The established assays for LSD1 activity[3,11] include peroxidase-based measurement of H_2O_2 production,[12] antibody-based estimation of demethylation products at lysine-4 of histone H3[13] and mass-spectrometry-based determination of substrate and/or products.[14,15] Most of these assays use recombinant LSD1 as the enzyme source and several synthetic peptides as the substrate. Several *N*-terminal truncated enzymes are used and are commercially available, because the *N*-terminal 184 residue region does not fold into an ordered well defined conformation[11] and the catalytic properties of the Δ184 truncated enzyme are indistinguishable from the activities of longer variants.[16] Forneris *et al.*[11] revealed that substrate recognition by LSD1 is not confined to the residues neighboring Lys-4 of histone H3, but the enzyme requires a sufficiently long peptide segment containing the *N*-terminal 20 amino acids of histone H3. Therefore, most of the assays published have used 21- or 25-mer *N*-terminal peptides that are dimethylated at Lys-4. Numerous assay

*To whom correspondence should be addressed.
E-mail: shidoji@sun.ac.jp

doi: 10.3164/jcbn.14-99

kits for screening of LSD1 inhibitors are now commercially available by using these substrates and the recombinant enzyme; however, no assay has revealed endogenous LSD1 enzyme activity in cellular extracts.

The present study describes an assay for measuring LSD1 activity with *N*-terminal 21-mer peptides of histone H3 using flow injection (FI) based time-of-flight mass spectrometry (TOF/MS). The reaction kinetics of LSD1 from this assay demonstrated typical consecutive kinetics of the demethylation reactions from the dimethylated substrate to the unmethylated product through a monomethylated intermediate in a single reaction tube without any pre- or post-treatment. The FI-TOF/MS assay for LSD1 activity is a novel, label-free approach and the detection of endogenous LSD1 enzyme activity in the nuclear extracts of cultured cells is straightforward.

Materials and Methods

Enzymes and substrates. Highly active recombinant human LSD1 (BML-SE544; hLSD1, aa151–852, 78 kDa, >20 U/μg protein, One U = 1 pmol demethylated/min at 30°C) was purchased from Enzo Life Sciences (Farmingdale, NY). The histone H3 amino-terminal 1–21 peptide with unmethylated Lys-4 or H3K4me0 (#61701), the histone H3 amino-terminal 1–21 peptide with monomethylated Lys-4 or H3K4me1 (#64459) and the histone H3 amino-terminal 1–21 peptide with dimethylated Lys-4 or H3K4me2 (#63677) were purchased from AnaSpec (Fremont, CA). These peptides were dissolved in deionized water and kept frozen at –20°C until use. Recombinant human monoamine oxidase-B (MAOB) (M7441, 15 U/mg protein, One U = 1 nmol deaminated/min at pH 7.4 and 37°C) and *trans*-2-phenylcyclopropylamine hydrochloride (2-PCPA) were purchased from Sigma-Aldrich (St. Louis, MO).

Enzyme reaction. A basic reaction mixture consisted of hLSD1 (250 ng = 3.2 pmol) and H3K4me2 (1 nmol) in 50 μl of assay buffer (50 mM Tris-HCl, pH 8.5, 5% glycerol) containing 0.1% bovine serum albumin. After gentle mixing of the reaction mixture on ice, the reactions were initiated by warming in a microtube at 30°C and incubation for 30 min or a designated period. The enzyme reactions were terminated by the addition of acetone at a final concentration of 80% (v/v). To perform precipitation of the peptides efficiently, the resultant acetone mixtures were incubated at room temperature for at least 1 h. The pellets obtained by centrifugation at 20,600 × *g* for 20 min were washed once with 15 mM ammonium hydroxide, and dissolved in water containing 0.05% trifluoroacetic acid (TFA) with sonication. After brief centrifugation, the resultant extracts were then filtered through a Millex-LG 0.2 μm (Merck Millipore, Darmstadt, Germany) for mass analysis.

Flow-injection for time-of-flight mass spectrometry (FI-TOF/MS). We quantitatively measured the LSD1 substrate, H3K4me2, as well as two products of the enzyme reaction, H3K4me1 and H3K4me0 by FI-TOF/MS. The flow rate of the mobile phase (acetonitrile/50 mM formic acid in water = 60/40) was 50 μl/min and was infused with a Waters Acquity UPLC system (Nihon Waters, Tokyo, Japan). Automated FI was performed in duplicate at an injection volume of 2 μl. The histone peptides were ionized by electrospray ionization (ESI) and were detected in a positive ion mode of the TOF/MS system (Waters^{R} Xevo^{TM} QTof MS, Nihon Waters), which was calibrated with sodium formate and lock-sprayed with Leu encephalin (Nihon Waters) each time. The optimal instrument parameters were as follows: a capillary voltage of 3.0 kV, a cone voltage of 30 V, a source temperature of 120°C, and a desolvation temperature of 350°C.

Kinetic analyses. Initial velocities (v_0) of hLSD1 were measured at 5 min and then plotted as a function of substrate concentration. The Michaelis-Menten equation (Eq. (1)) was fit to the data using the Prism 6 software (GraphPad Software, San Diego, CA) to calculate the k_{cat} and K_m values:

$$v_0 = k_{cat}[E_{total}] \times [S]/(K_m + [S]) \quad (1)$$

where $[E_{total}]$ represents the concentration of the enzyme used and [S] represents the concentrations of H3K4me2 added to the reaction mixture.

LSD1 is a catalyst for consecutive demethylation reactions from H3K4me2 to H3K4me1 and from H3K4me1 to H3K4me0. The first order reaction consists of two consecutive, irreversible elementary steps:

$$\text{H3K4me2} \xrightarrow{(k_1)} \text{H3K4me1} \xrightarrow{(k_2)} \text{H3K4me0} \quad (2)$$

where k_1 and k_2 are rate constants for each step. When the reaction starts with an initial concentration of $[H3K4me2]_0$, the concentrations of both H3K4me1 and H3K4me0 are zero. The expected concentrations of the three histone-H3 peptides are expressed as a function of time as follows:

$$[H3K4me2] = [H3K4me2]_0 \times \exp(-k_1 t) \quad (3)$$

$$[H3K4me1] = [H3K4me2]_0 \times k_1/(k_2 - k_1)\{\exp(-k_1 t) - \exp(-k_2 t)\} \quad (4)$$

$$[H3K4me0] = [H3K4me2]_0 \times (1 + \{k_1\exp(-k_2 t) - k_2\exp(-k_1 t)\}/(k_2 - k_1)) \quad (5)$$

$$[H3K4me2]_0 = [H3K4me2] + [H3K4me1] + [H3K4me0] \quad (6)$$

The time-course experimental data were applied with nonlinear regression to fit a consecutive reaction model with equations (3), (4) and (5) using the Prism 6 software to calculate the k_1 and k_2 values.

Preparation of nuclear extracts. The human neuroblastoma-derived SH-SY5Y cell line was obtained from ATCC (Manassas, VA), and human adenocarcinoma HeLa and human prostate tumor PC-3 cell lines were provided by the RIKEN BRC (Tsukuba, Japan). SH-SY5Y and HeLa cells were cultured in D-MEM (4,500 mg/L glucose, Wako Pure Chem. Ind., Ltd., Osaka, Japan) and PC-3 cells were cultured in RPMI-1640 (Wako Pure Chem.) supplemented with 10% heat-inactivated fetal bovine serum (Thermo Scientific Hyclone, Yokohama, Japan). At 80% confluence, cells were detached by a cell lifter and suspended in ice-cold phosphate buffered saline containing 1 mM phenylmethanesulfonyl fluoride (PMSF, Sigma Aldrich). Nuclear extracts were then prepared by the following procedures. The detached cells were collected by centrifuge at 300 × *g* for 5 min, and cells were washed with a resuspension buffer (10 mM Tris-HCl, pH 8.0, 10 mM KCl, 3 mM $MgCl_2$, protease inhibitor cocktail [cOmplete Mini, Roche Diagnostics K.K., Tokyo, Japan], 1 mM PMSF and 0.5 mM dithiothreitol [DTT]). The cells were resuspended in the resuspension buffer containing 0.1% NP-40. After incubation on ice for 10–20 min, the nuclei were visually confirmed under the microscope. After centrifugation at 550 × *g* for 5 min, the nuclei were washed with the resuspension buffer. The nuclear pellets were resuspended with the assay buffer containing cOmplete Mini, 1 mM PMSF and 0.5 mM DTT, and homogenized by sonication (10 s × 6, interval = 30 s, amplitude = 20%) with a Sonifier 250 (Branson Ultrasonics Corporation, Danbury, CT). After centrifugation (20,600 × *g*, 20 min), the supernatant was kept as nuclear extracts. The protein concentrations were measured with the *DC* Protein Assay kit (Bio-Rad Laboratories, Hercules, CA). The nuclear extracts were used as an enzyme source in place of the recombinant hLSD1 for the FI-TOF/MS LSD1 assay described above.

doi: 10.3164/jcbn.14-99

Immunoblotting. The nuclear extracts (4 μg protein equiv.) were denatured in 6× sample buffer (0.4 M Tris-HCl, pH 6.8, 12% SDS, 45% glycerol, 0.024% bromophenol blue and 10% 2-mercaptoethanol) by boiling at 95°C for 5 min, resolved by SDS-PAGE and transferred to a PVDF membrane. The membrane was incubated with a polyclonal anti-LSD1 antibody (1:1000, #2139, Cell Signaling Technology, Danvers, MA). Luminescence was produced by incubation with the SuperSignal West Femto Maximum Sensitivity Substrate (Thermo Scientific, Rockford, IL) and detected by using a LAS-1000 imaging system (GE Healthcare Japan, Tokyo, Japan). Collected images were analyzed by the ImageJ software (U.S. National Institutes of Health, Bethesda, MD).

Results and Discussion

FI-TOF/MS assay development. Initially, the identification of positive ions from the substrate H3K4me2 by FI-TOF/MS was performed. The accurate monoisotopic mass of H3K4me2 is calculated to be 2281.346 from its molecular formula ($^{12}C_{96}{}^{1}H_{176}{}^{14}N_{36}{}^{16}O_{28}$). This 21-mer peptide contains seven basic amino acids (i.e., 3 Arg and 4 Lys residues). Under acidic conditions with 0.05% TFA by volume, the peptide can be easily protonated at multiple sites and independent and different protonated multivalent ions are calculated as follows: $[M + 3H^+]^{3+}$, m/z = 761.456; $[M + 4H^+]^{4+}$, m/z = 571.344; $[M + 5H^+]^{5+}$, m/z = 457.277; $[M + 6H^+]^{6+}$, m/z = 381.232; $[M + 7H^+]^{7+}$, m/z = 326.914. When we injected the H3K4me2 alone with 0.05% TFA, four major mass peaks were detected between 300 and 800 m/z[+] on the mass spectrum. As shown in Fig. 1A, the accurate masses (m/z) of the four major peaks were determined to be 761.455, 571.342, 457.274 and 381.225, which exactly corresponded to the above-described calculated values of $[M + 3H^+]^{3+}$, $[M + 4H^+]^{4+}$, $[M + 5H^+]^{5+}$ and $[M + 6H^+]^{6+}$, respectively. A tiny mass peak (m/z = 326.910) corresponding to the $[M + 7H^+]^{7+}$ species was detected; although Plant *et al.*[14] demonstrated using a RapidFire tandem mass spectrometry (MS/MS) approach that $[M + 7H^+]^{7+}$ and $[M + 8H^+]^{8+}$ ion species are observable in addition to the $[M + 3H^+]^{3+}$, $[M + 4H^+]^{4+}$, $[M + 5H^+]^{5+}$ and $[M + 6H^+]^{6+}$ species. This difference is presumably because their peptide H3K4me2

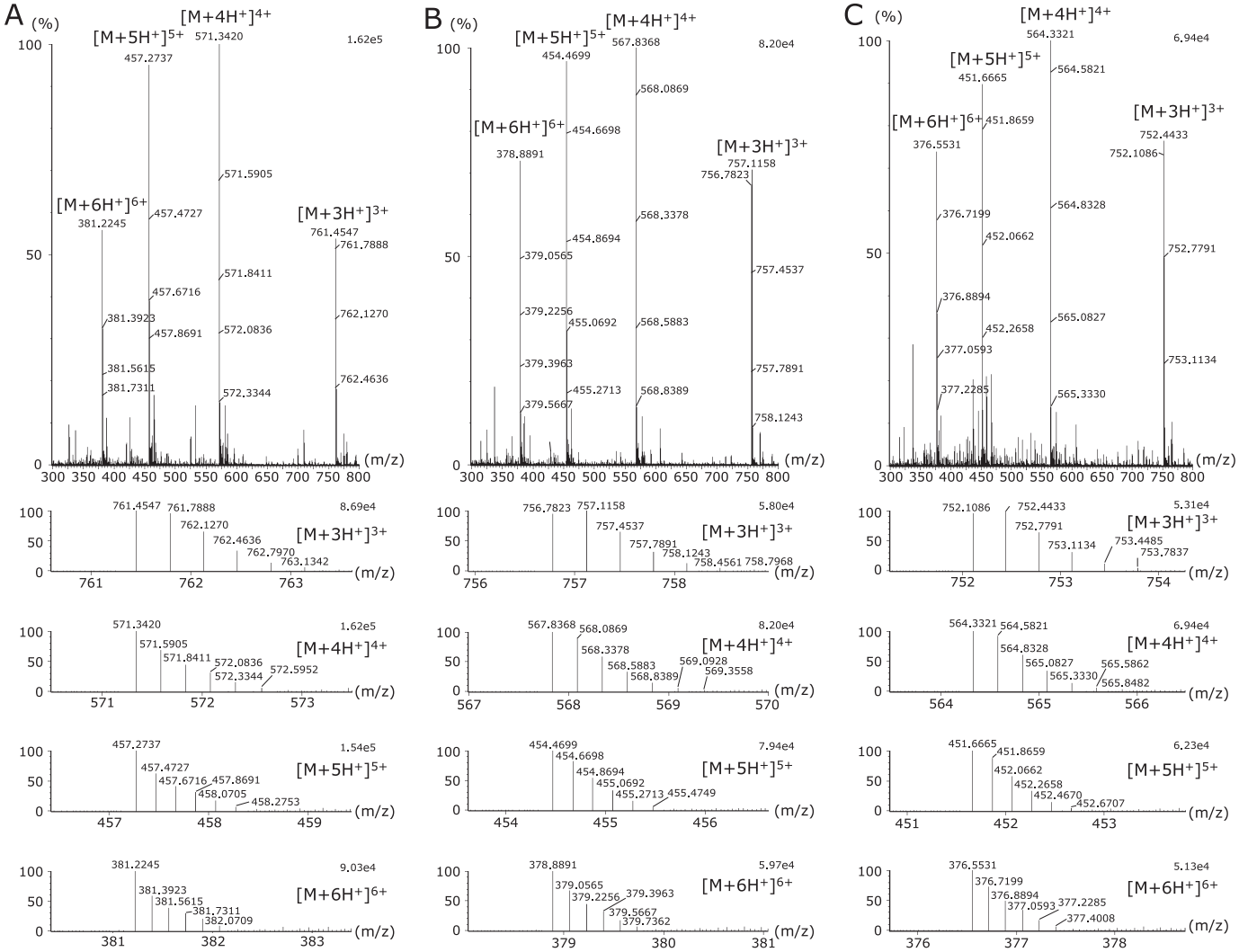

Fig. 1. Analysis of dimethyl(K4)-histone H3 (1–21) peptide by time-of-flight mass spectrometry. Commercially available H3K4 peptides were dissolved in assay buffer and precipitated by acetone followed by solvent replacement to ultra-pure water containing 0.05% TFA to a final concentration of 20 μM H3K4me2 (A), 13.6 μM H3K4me1 (B) or 14.8 μM H3K4me0 (C), and filtered through Millex-LG, 0.2 μm prior to injection onto the TOF/MS apparatus. Positive ions were recorded from 50 to 1,000 m/z and are shown from 300 to 800 (the upper half). $[M + 3H^+]^{3+}$, $[M + 4H^+]^{4+}$, $[M + 5H^+]^{5+}$ and $[M + 6H^+]^{6+}$ represent mass peaks corresponding to the theoretically-calculated m/z. The detailed mass spectra of $[M + 3H^+]^{3+}$, $[M + 4H^+]^{4+}$, $[M + 5H^+]^{5+}$ and $[M + 6H^+]^{6+}$ are shown as each isotopic envelop (the lower half).

(1–25) contains one more Lys residue than our H3K4me2 (1–21) peptide.

The above-mentioned four major ion species found in the present study formed as an isotopic envelope as shown in the lower half of panel A of Fig. 1. In other words, the putative $[M + nH^+]^{n+}$ (n = 3–6) ions were surrounded with several equally spaced ions at a given "n" on each mass spectrum, so that a trivalent ion cluster gave a 0.33 m/z interval, the tetravalent ion gave an m/z interval of 0.25, the pentavalent ion gave an m/z interval of 0.20 and the hexavalent ion gave a m/z interval of 0.17. These numbers all sum to 1.0 if each interval is multiplied by their respective valency, suggesting that these clusters consist of isotopic equivalent ions containing additional neutrons to varying degrees. Therefore, we tentatively assigned $[M + 3H^+]^{3+}$, $[M + 4H^+]^{4+}$, $[M + 5H^+]^{5+}$ and $[M + 6H^+]^{6+}$ to four major ions of H3K4me2. Similar results were obtained with either H3K4me1 or H3K4me0 (Fig. 1B and C).

Although multiple species of ions from H3K4me2 were detected with different abundance, quantitative measurement was conducted with increasing amounts (0–40 pmol) of the peptide. Monitoring the tentative tetravalent ions, $[M + 4H^+]^{4+}$, in combination with the isotopic envelope gave a straight line (y = 74.39x, R^2 = 0.9835, Fig. 2A). Similar results on the linearity of standard curves were obtained with the pentavalent ion envelope, but the trivalent and hexavalent ion envelopes gave shallower slopes (Fig. 2A). The same observations were true with both H3K4me1 and H3K4me0, but the ionization efficiency was clearly dependent on the methylation status; the unmethylated peptide was less efficiently ionized than both methylated peptides (Fig. 2B and C).

Monitoring hLSD1 reactions by FI-TOF/MS. We then analyzed the positive mass ions in the reaction mixture containing the hLSD1 substrate and its products after acetone precipitation followed by solubilization in water containing 0.05% TFA (Fig. 3). Fig. 3A clearly shows that prior to the hLSD1 reaction only the substrate ions from the H3K4me2 peptide were detected as a characteristic isotopic envelope of the tetravalent ions in the

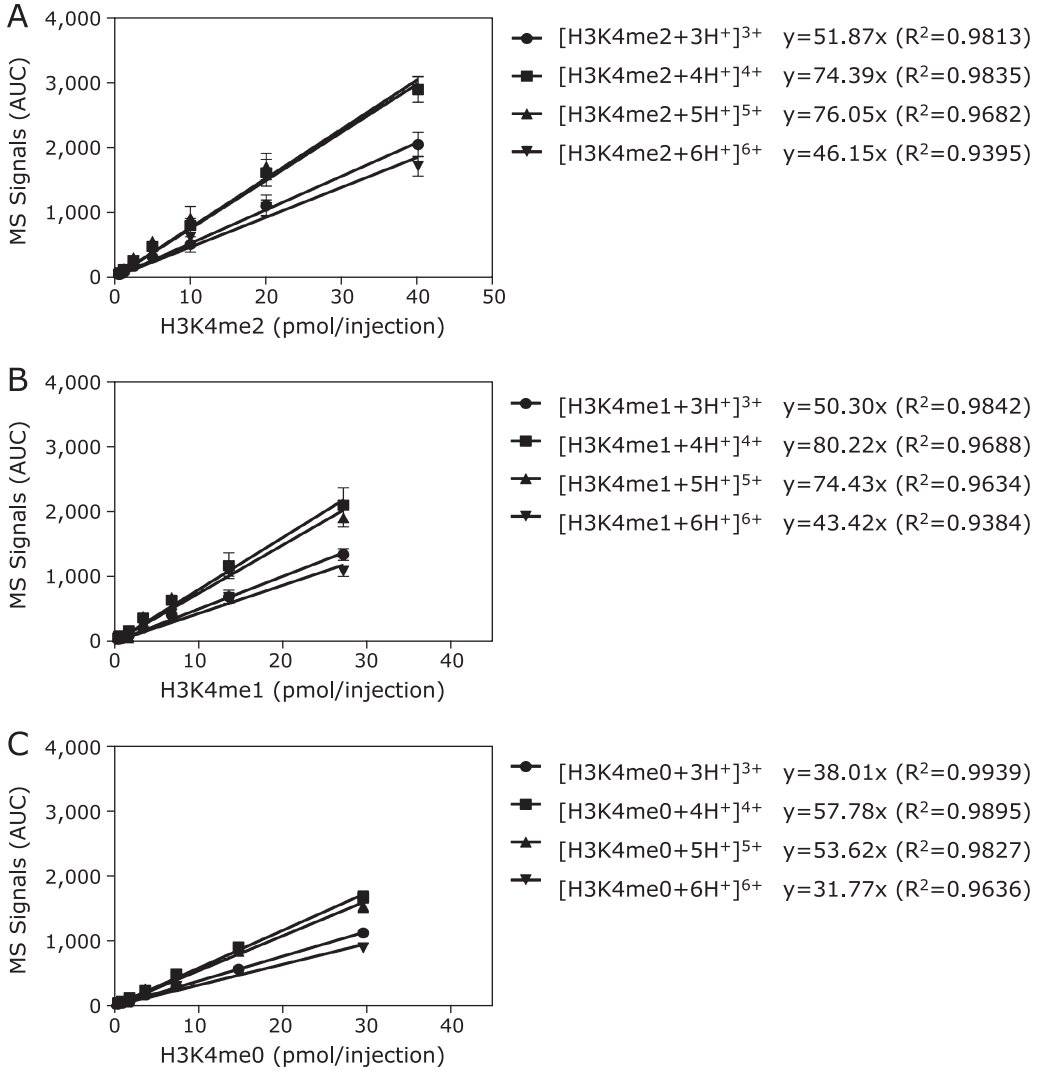

Fig. 2. Quantitative analyses of dimethyl(K4)-, monomethyl(K4)- and unmethyl(K4)-histone H3 (1–21) peptides by flow-injection time-of-flight mass spectrometry (FI-TOF/MS). Commercially available H3K4me2 (A), H3K4me1 (B) or H3K4me0 (C) peptides were dissolved in assay buffer and precipitated with acetone followed by solvent replacement to ultra-pure water containing 0.05% TFA and filtered through Millex-LG, 0.2 μm prior to injection onto the TOF/MS apparatus. Positive ions of the injected samples (2 μl each) were recorded from 50 to 1,000 m/z. Four major ions of the trivalent ion cluster ($[M + 3H^+]^{3+}$, closed circle), the tetravalent ion cluster ($[M + 4H^+]^{4+}$, closed square), the pentavalent ion cluster ($[M + 5H^+]^{5+}$, closed triangle) and the hexavalent ion cluster ($[M + 6H^+]^{6+}$, closed inverted triangle) were integrated to measure each ion. Signal intensities of each MS were plotted against the amounts of the injected peptide. Linear fittings are shown with the regression formula (y = ax) and the goodness of fitting (R^2).

doi: 10.3164/jcbn.14-99

range of 560 to 575 m/z(+). The total MS signals of the tetravalent ions detected were ~60% of the MS signals from an equi-amount of the pure substrate precipitated by acetone and then dissolved in water containing 0.05% TFA, indicating that some ion suppression caused by matrix effects of the enzyme solution did occur.[18] However, as discussed in detail below, the putative matrix effects were not variable during the enzyme reaction such that the MS signals of H3K4me2 from the reaction mixture were quantitative.

Twenty minutes after the enzyme reaction started two other isotopic envelopes appeared at around 567.840 and 564.336 m/z, corresponding to $[H3K4me1 + 4H^+]^{4+}$ and $[H3K4me0 + 4H^+]^{4+}$, respectively (Fig. 3B). Indeed, the differences in m/z between these three isotopic envelopes in panel B were 3.504, which is the number that exactly corresponds to the monoisotopic mass number of $^{12}C^1H_2$ divided by the valency of four. When the enzyme reaction proceeded to 120 min the amount of the final product, unmethylated $[H3K4me0]^{4+}$, had accumulated, whereas the amount of the substrate $[H3K4me2]^{4+}$ had decreased. The intermediate product $[H3K4me1]^{4+}$ had also decreased in amount (Fig. 3C). Among the multivalent ions from H3K4me2, H3K4me1 and H3K4me0, we decided to monitor the tetravalent ions from the histone peptides to trace the LSD1 reactions, because the tetravalent ions of the three molecular species were more efficiently detected than the tri-, penta- and hexavalent ions (Fig. 1A and 2).

Simulation analysis of the consecutive reactions.

Fig. 3D clearly shows an hLSD1 reaction time course of a typical

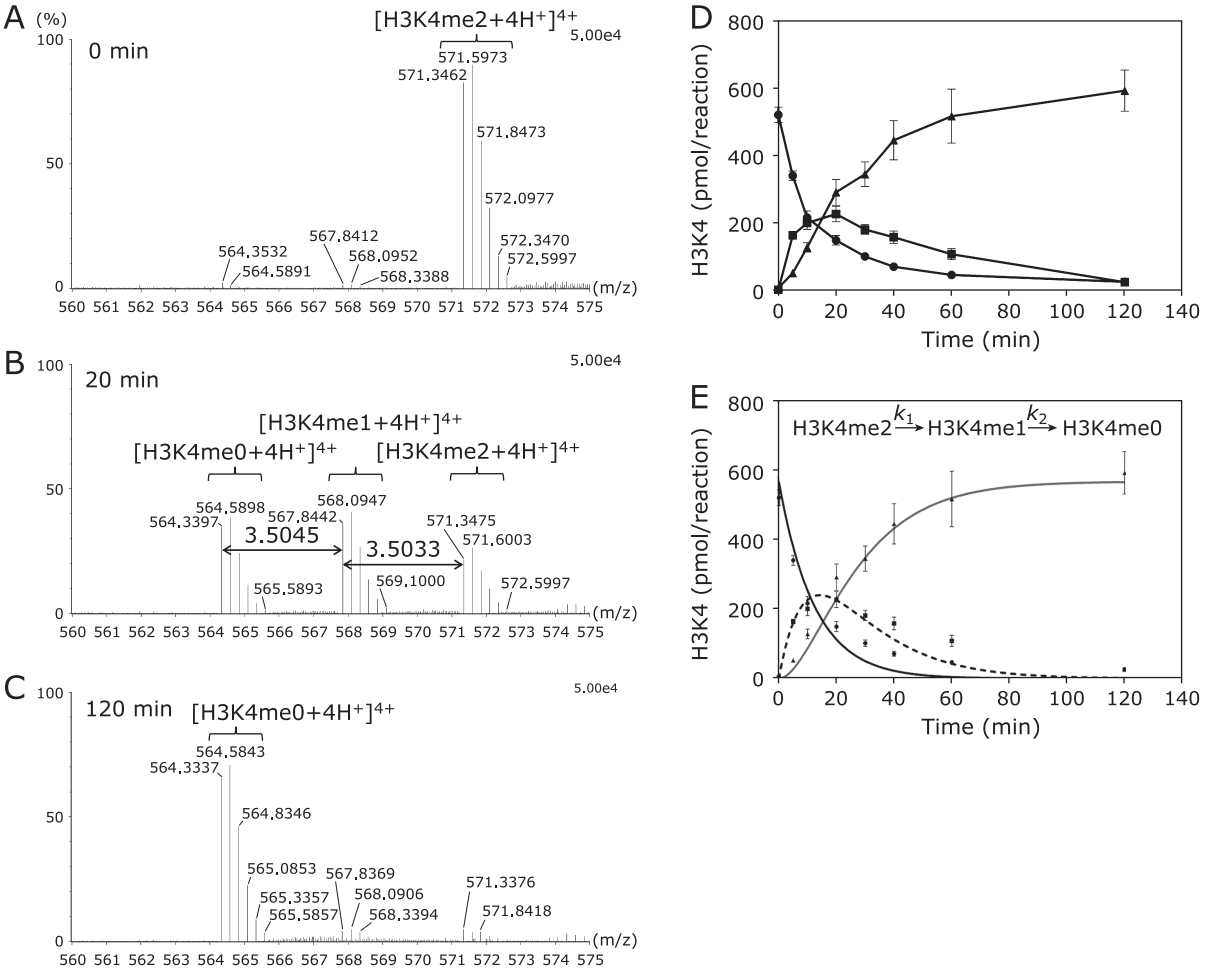

Fig. 3. Detection of monomethyl(K4)- and unmethyl(K4)-histone H3 (1–21) peptides after the LSD1 reaction. (A) Positive ion mass spectrum of the acetone-treated extract (2 μl injected) from a reaction mixture (50 μl) of H3K4me2 (1 nmol) with hLSD1 (3.2 pmol), which was recorded prior to incubation at 30°C. The tetravalent H3K4me2 isotopic envelope was detected at m/z of 571–573. (B) Positive ion mass spectrum of the acetone-treated extract (2 μl injected) from a reaction mixture (50 μl) of H3K4me2 (1 nmol) with hLSD1 (3.2 pmol), which was recorded 20 min after the reaction had started. The tetravalent H3K4me1 ion cluster was smaller than H3K4me2 by 3.50 m/z, which corresponds to an m/z of $(CH_2)/4$. The $[H3K4me0]^{4+}$ ion cluster was smaller by a further 3.50 m/z. (C) The positive ion mass spectrum of the acetone-treated extract (2 μl injected) from a reaction mixture (50 μl) of H3K4me2 (1 nmol) with hLSD1 (3.2 pmol), which was recorded at 120 min after the reaction started. (D) Typical consecutive reaction kinetics from H3K4me2 to H3K4me0 through H3K4me1 catalyzed by hLSD1 revealed by FI-TOF/MS. H3K4me2 (1 nmol) was incubated with hLSD1 (3.2 pmol) at 30°C. At the indicated time points, the reaction was terminated by adding 4 vol. of acetone and the resultant precipitates were extracted in a 0.05% TFA solution. After filtration through Millex-LG 0.2 μm, FI-TOF/MS was conducted to measure the amounts of H3K4me2 (●), H3K4me1 (■) and H3K4me0 (▲) by integration of each of the major tetravalent ions (four of them). The peak areas (AUC) of each MS signal on the mass chromatogram were plotted against the reaction time. Data are expressed as mean ± SD (n = 3). (E) Typical consecutive reaction kinetics from H3K4me2 to H3K4me0 through H3K4me1 catalyzed by hLSD1 revealed by FI-TOF/MS. By using the data shown in panel E, a simulation of first-order consecutive reaction kinetics was performed by GraphPad Prism 6, which was installed with Equations "(3); $[H3K4me2] = [H3K4me2]_0 \times \exp(-k_1t)$", "(4); $[H3K4me1] = [H3K4me2]_0 \times k_1/(k_2 - k_1)\{\exp(-k_1t) - \exp(-k_2t)\}$" and "(5); $[H3K4me0] = [H3K4me2]_0 \times (1 + \{k_1\exp(k_2t) - k_2\exp(-k_1t)\}/(k_2 - k_1))$", indicating exponential decay, transient peak and sigmoidal accumulation curves in each molecular species such as H3K4me2 (●), H3K4me1 (■) and H3K4me0 (▲). The amounts (pmol/reaction) of each species were plotted against the reaction time. Data are expressed as mean ± SD (n = 3).

consecutive-type reaction in which the substrate H3K4me2 is converted to the product H3K4me0 through an intermediate H3K4me1, as monitored by their tetravalent ions. The substrate H3K4me2 was observed to decay exponentially and the intermediate product H3K4me1 transiently increased exponentially to a maximum after 20 min reaction time and then gradually decreased, whereas the final product H3K4me0 gradually accumulated in a sigmoidal fashion.

We then performed a nonlinear global simulation of these reaction time-course data using Equations (3), (4) and (5) with the GraphPad Prism 6 software to calculate k_1 and k_2. As a result, k_1 ($8.08 \times 10^{-2} \pm 4.52 \times 10^{-3}$ pmol/min) was slightly larger than k_2 ($6.02 \times 10^{-2} \pm 3.82 \times 10^{-3}$ pmol/min) with a high goodness ($R^2 = 0.9404$) of fit to a first-order consecutive reactions model (nonlinear fitting by GraphPad Prism 6, Fig. 3E).

Plant *et al.*[14] also demonstrated a time course of the recombinant LSD1 reaction by monitoring three histone H3 (1–25) peptides with a label-free MS/MS assay; however, they showed a linear rather than an exponential decay of H3K4me2 (1–25) until 120 min. Their results were quite different from the results presented herein, despite both groups using similar enzymes of *N*-truncated recombinant human LSD1 (171–852 or 151–852 hLSD1) and similar synthetic *N*-terminal H3K4me2 peptide substrates (1–25 or 1–21 histone H3). Major differences in the conditions between the assays are the concentrations of hLSD1 (2.5 nM vs 64 nM) and H3K4me2 (0.27 μM vs 20 μM), and the resultant ratios of the substrate to the enzyme (108 vs 312.5), which may explain the different kinetics between the previous report and the results herein.

Michaelis-Menten constants of the hLSD1 reaction. The initial velocity (v_0) of formation of H3K4me1 + H3K4me0 from H3K4me2 was plotted against the concentrations of H3K4me2 added (Fig. 4A). A typical Michaelis-Menten-type saturation curve was obtained, and the parameters of k_{cat} and K_m were found to be 15.8 min^{-1} and 3.08 μM, respectively, and the value of k_{cat}/K_m was calculated to be 5.12 $min^{-1} \cdot \mu M^{-1}$. These values for the H3K4me2 *N*-terminal 1–21 peptide are in reasonable agreement with the values reported previously by Forneris *et al.*[16]

The same kinetics analysis describing the formation of H3K4me0 from H3K4me1 was performed with hLSD1 (Fig. 4B). As a result, a Prism 6 simulation revealed that k_{cat} was 7.68 min^{-1}, K_m was 0.70 μM and k_{cat}/K_m was 10.97 $min^{-1} \cdot \mu M^{-1}$ for the demethylation reaction of H3K4me1. Although k_{cat} and the catalytic efficiency (k_{cat}/K_m) of the second reaction were in the same range as those of the first reaction, we have not resolved how efficiently LSD1 catalyze a sequential demethylation of H3K4me1 produced from H3K4me2 on the catalytic site of the enzyme. The enzyme-produced H3K4me1 may not be extensively distributed in the reaction mixture, which may cause a higher catalytic efficiency than the measured catalytic efficiency for the second reaction.

Inhibitory effects of 2-PCPA on hLSD1 activity. To validate the presented FI-TOF/MS assay for measuring hLSD1 activity, we used 2-PCPA, a benchmark inhibitor over a concentration range of 0–100 μM in a reaction mixture (50 μl) containing H3K4me2 (1 nmol) and hLSD1 (3.2 pmol). As shown in Fig. 5A, 2-PCPA inhibited hLSD1-catalyzed production of H3K4me1 and H3K4me0 in a dose-dependent manner with an IC_{50} (half maximal inhibitory concentration) of 6.90 μM. In the literature, the reported

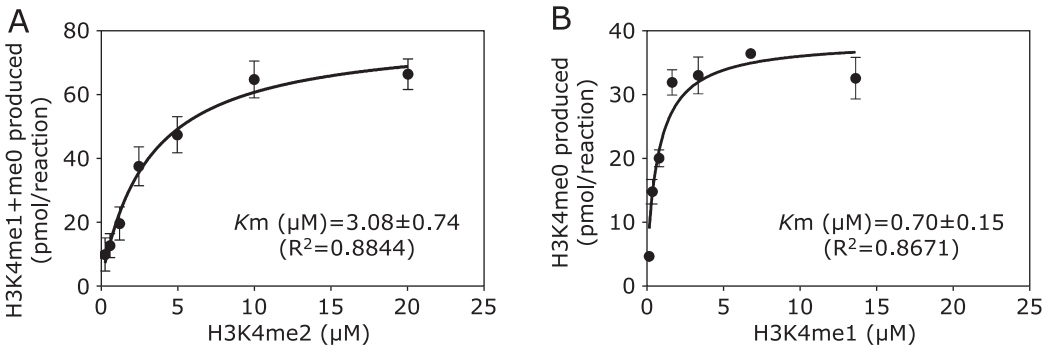

Fig. 4. Saturation curves of the hLSD1 activity with increasing concentrations of H3K4me2 (A), or H3K4me1 (B). Increasing concentrations of H3K4me2 (0.3–20 μM) or H3K4me1 (0.2–13.6 μM) were incubated with hLSD1 (3.2 pmol = 250 ng) at 30°C for 5 min. The LSD1 activity was expressed by the amount of H3K4me1 + H3K4me0 (A) or H3K4me0 (B) produced by the enzyme reaction. Each curve was drawn after fitting to the Prism 6-preinstalled Michaelis-Menten equation. Data are expressed as mean ± SD (n = 3).

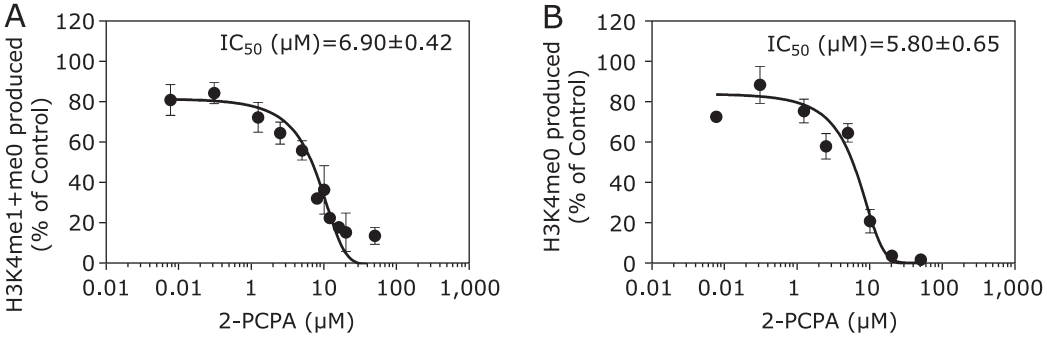

Fig. 5. Inhibition of the hLSD1 activity by increasing concentrations of 2-PCPA demonstrated by FI-TOF/MS. Increasing concentrations (0.08–50 μM) of 2-PCPA were preincubated on ice for 30 min with hLSD1 (250 ng), and then, the enzyme reaction started by adding either (A) H3K4me2 (1 nmol), or (B) H3K4me1 (1 nmol), and warming at 30°C. The initial velocity of the enzyme reaction was measured at 5 min and expressed as the produced amounts of H3K4me1 + H3K4me0. Curve fitting was performed using GraphPad Prism 6. Data are expressed as mean ± SD (n = 3).

doi: 10.3164/jcbn.14-99

IC_{50} of 2-PCPA for LSD1 is in the range from <2 to 34 μM with the substrate concentrations from 0.27 to 67 μM.[14,19,20]

When we drew focus to the production of H3K4me0 from H3K4me1, the IC_{50} of 2-PCPA was found to be 5.80 μM (Fig. 5B). Although the second demethylation reaction appears to be more sensitive to 2-PCPA, we cannot directly compare the IC_{50} value for the second reaction with that of the first reaction. Inasmuch as 2-PCPA, a well-established suicide substrate for LSD1, covalently binds to FAD of LSD1, the two consecutive reactions should be both affected by 2-PCPA.

Measurement of the endogenous LSD1 activity in the nuclear extracts of cultured cells. To apply the presented FI-TOF/MS assay for measuring endogenous LSD1 activity in cells, we prepared nuclear extracts from three different human cell lines,

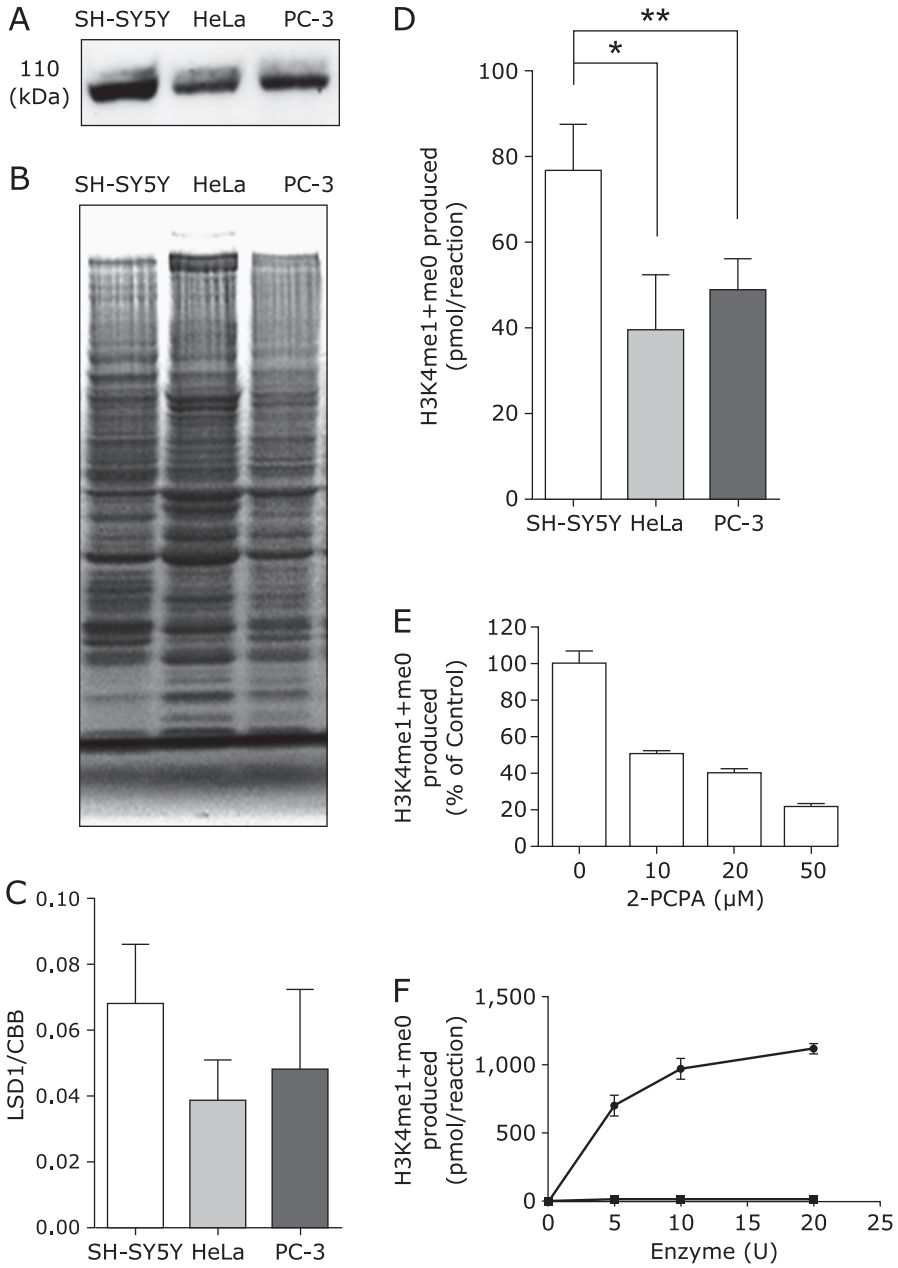

Fig. 6. Detection of LSD1 activity in the nuclear extracts of cultured cells. (A) Each nuclear extract (4 μg protein each per lane) was applied onto the SDS-PAGE and LSD1 proteins were detected with an anti-LSD1 antibody. (B) Total protein staining of the SDS-PAGE gel for the nuclear extracts of cultured cells. Nuclear extracts of SH-SY5Y, HeLa and PC-3 cells (4 μg protein equiv. per each lane) were separated by SDS-PAGE, and total proteins in a gel were stained with Coomassie brilliant blue dye. (C) The density of the LSD1 bands was quantified by ImageJ. The measured LSD1 levels were expressed relative to the density of total protein per each lane in the same gel stained with Coomassie brilliant blue (CBB) dye. Data represent means ± SD (n = 6 for SH-SY5Y, n = 4 for HeLa and PC-3). (D) H3K4me2 (1 nmol) was incubated with nuclei extracts (each 10 μg protein) at 30°C for 1 h. LSD1 activity expressed by the amount of H3K4me1 + H3K4me0 produced by the nuclear enzyme. Data were expressed as mean ± SD (n = 4 for SH-SY5Y, n = 3 for HeLa and PC-3). *p<0.05, **p<0.01. (E) The nuclear extracts of SH-SY5Y cells (10 μg protein) were preincubated on ice with 2-PCPA for 1 h, and then, the enzyme reaction started by adding H3K4me2 (1 nmol) and warming at 30°C. The initial velocity of the enzyme reaction was measured at 1 h and expressed as the produced amount of H3K4me1 + H3K4me0. Data were expressed as mean ± SD (n = 3). (F) Inability of hMAOB to catalyze the demetylation of dimethyl(K4)-histone H3 (1-21) peptide. H3K4me2 (1 nmol) was incubated with the increasing amounts (0–20 U) of hLSD1 (●) or hMAOB (■) at 30°C for 1 h. FI-TOF/MS was conducted to measure the product amounts of H3K4me1 + H3K4me0.

because LSD1 is recognized as a nuclear marker protein.[3] A major 110-kDa band was detected in the nuclear extracts derived from the three cell lines tested (Fig. 6A). The cellular amount of LSD1 protein relative to Coomassie blue-stained proteins (Fig. 6B) was the highest in SH-SY5Y cells and the lowest in HeLa cells (Fig. 6C). In accordance with these immunoblotting data, the FI-TOF/MS assay revealed that the endogenous LSD1 activity was higher in the nuclear extracts of SH-SY5Y cells than those of HeLa or PC-3 cells (Fig. 6D). As shown in Fig. 6E, the endogenous LSD1 activity was inhibited dose-dependently with 2-PCPA, which is also able to inhibit MAOB, a mitochondrial flavoenzyme. However, we confirmed that recombinant hMAOB was unable to catalyze the demethylation reaction of H3K4me2 (Fig. 6F), suggesting that 2-PCPA inhibition in the nuclear extracts of SH-SY5Y cells is a manifestation of the nuclear-localized active LSD1 enzyme. However, we cannot exclude the possibility that some other endogenous enzymes may be involved in demethylation reactions in our assay. The only one paralogue of LSD1 so far reported is LSD2/KDM1B, which is able to demethylate a substrate of H3K4me2 (1–21) peptide, but not H3R2me1K4me1 (1–21) peptide that is a substrate for LSD1.[7] But, the remaining 20% activity at 50 μM 2-PCPA (Fig. 6E) could not be provided by a putative LSD2 in SH-SY5Y cells, because LSD2 is also sensitive to 2-PCPA treatment.[7] The expression profiles of LSD2 have now been scarcely available in the literatures so that we have no information about endogenous LSD2 activity in SH-SY5Y cells. In the immediate future, H3R2me1K4me1 will be commercially available and can be utilized for more specific assay of LSD1 activity.

Finally, it is worthwhile to mention that the LSD1 enzyme activity could be modulated by the protein-protein interaction with other nuclear proteins such as CoREST, NuRD,[21] nuclear transcription factors (estrogen receptor and androgen receptor)[22] and HDAC.[23] Furthermore, some small-molecular agents such as resveratrol and curcumin were reported to inhibit LSD1 activity.[24] We recently also found that several acyclic diterpenoids directly inhibit recombinant human LSD1 activity at their micromolar concentrations.[25] Therefore, we must be careful to assess the epigenetic role of LSD1, the enzyme activity of which may not correlate its protein levels evaluated by western blotting.

In conclusion, the present study describes a novel assay for LSD1 activity using FI-TOF/MS, and an *N*-terminal 21-mer peptide of histone H3 with methylated Lys-4. The assay revealed typical first-order consecutive kinetics of the demethylation reactions, in which the dimethylated substrate is converted to the unmethylated product through a monomethylated intermediate in a single reaction tube without any pre- or post-treatment requirements. Furthermore, the FI-TOF/MS assay for LSD1 unequivocally detected the enzyme activity in the nuclear extracts of three human cell lines.

Acknowledgments

This work was financially supported by the research fund, Project Research Fund of the University of Nagasaki, Japan.

Abbreviations

AUC	area under the curve
ESI	electrospray ionization
FI	flow-injection
H3K4me0	histone H3 amino-terminal 1–21 peptide with unmethylated lysine-4
H3K4me1	histone H3 amino-terminal 1–21 peptide with monomethylated lysine-4
H3K4me2	histone H3 amino-terminal 1–21 peptide with dimethylated lysine-4
IC_{50}	half maximal inhibitory concentration
KDM	lysine-specific demethylase
LSD1	lysine-specific demethylase 1
MS/MS	tandem mass spectrometry
2-PCPA	*trans*-2-phenylcyclopropylamine or tranylcypromine
TFA	trifluroacetic acid
TOF/MS	time-of-flight mass spectrometry

Conflict of Interest

No potential conflicts of interest were disclosed.

References

1 Kaur P, Shorey LE, Ho E, Dashwood RH, Williams DE. The epigenome as a potential mediator of cancer and disease prevention in prenatal development. *Nutr Rev* 2014; **71**: 441–457.
2 Campbell RM, Tummino PJ. Cancer epigenetics drug discovery and development: the challenge of hitting the mark. *J Clin Invest* 2014; **124**: 64–69.
3 Shi Y, Lan F, Matson C, *et al*. Histone demethylation mediated by the nuclear amine oxidase homolog LSD1. *Cell* 2004; **119**: 941–953.
4 Forneris F, Battaglioli E, Mattevi A, Binda C. New roles of flavoproteins in molecular cell biology: histone demethylase LSD1 and chromatin. *FEBS J* 2009; **276**: 4304–4312.
5 Mimasu S, Sengoku T, Fukuzawa S, Umehara T, Yokoyama S. Crystal structure of histone demethylase LSD1 and tranylcypromine at 2.25 A. *Biochem Biophys Res Commun* 2008; **366**: 15–22.
6 Schmidt DM, McCafferty DG. *trans*-2-Phenylcyclopropylamine is a mechanism-based inactivator of the histone demethylase LSD1. *Biochemistry* 2007; **46**: 4408–4416.
7 Karytinos A, Forneris F, Profumo A, *et al*. A novel mammalian flavin-dependent histone demethylase. *J Biol Chem* 2009; **284**: 17775–17782.
8 Ciccone DN, Su H, Hevi S, *et al*. KDM1B is a histone H3K4 demethylase required to establish maternal genomic imprints. *Nature* 2009; **461**: 415–418.
9 Schulte JH, Lim S, Schramm A, *et al*. Lysine-specific demethylase 1 is strongly expressed in poorly differentiated neuroblastoma: implications for therapy. *Cancer Res* 2009; **69**: 2065–2071.
10 Schenk T, Chen WC, Gollner S, *et al*. Inhibition of the LSD1 (KDM1A) demethylase reactivates the all-trans-retinoic acid differentiation pathway in acute myeloid leukemia. *Nat Med* 2012; **18**: 605–611.
11 Forneris F, Binda C, Vanoni MA, Mattevi A, Battaglioli E. Histone demethylation catalysed by LSD1 is a flavin-dependent oxidative process. *FEBS Lett* 2005; **579**: 2203–2207.
12 Wang C, Caron M, Burdick D, *et al*. A sensitive, homogeneous, and high-throughput assay for lysine-specific histone demethylases at the H3K4 site. *Assay Drug Dev Technol* 2012; **10**: 179–186.
13 Tsukada Y, Nakayama KI. *In vitro* histone demethylase assay. *Cold Spring Harb Protoc* 2010; **2010**: pdb.prot5512.
14 Plant M, Dineen T, Cheng A, Long AM, Chen H, Morgenstern KA. Screening for lysine-specific demethylase-1 inhibitors using a label-free high-throughput mass spectrometry assay. *Anal Biochem* 2011; **419**: 217–227.
15 Blair LP, Avaritt NL, Huang R, Cole PA, Taverna SD, Tackett AJ. MassSQUIRM: An assay for quantitative measurement of lysine demethylase activity. *Epigenetics* 2011; **6**: 490–499.
16 Forneris F, Binda C, Vanoni MA, Battaglioli E, Mattevi A. Human histone demethylase LSD1 reads the histone code. *J Biol Chem* 2005; **280**: 41360–41365.
17 Chen X, Turecek F. The arginine anomaly: arginine radicals are poor hydrogen atom donors in electron transfer induced dissociations. *J Am Chem Soc* 2006; **128**: 12520–12530.
18 Fuhrer T, Heer D, Begemann B, Zamboni N. High-throughput, accurate mass metabolome profiling of cellular extracts by flow injection-time-of-flight mass spectrometry. *Anal Chem* 2011; **83**: 7074–7080.
19 Lee MG, Wynder C, Schmidt DM, McCafferty DG, Shiekhattar R. Histone H3 lysine 4 demethylation is a target of nonselective antidepressive medications. *Chem Biol* 2006; **13**: 563–567.
20 Benelkebir H, Hodgkinson C, Duriez PJ, *et al*. Enantioselective synthesis of tranylcypromine analogues as lysine demethylase (LSD1) inhibitors. *Bioorg*

doi: 10.3164/jcbn.14-99

Med Chem 2011; **19**: 3709–3716.
21 Cui S, Kolodziej KE, Obara N, *et al*. Nuclear receptors TR2 and TR4 recruit multiple epigenetic transcriptional corepressors that associate specifically with the embryonic β-type globin promoters in differentiated adult erythroid cells. *Mol Cell Biol* 2011; **31**: 3298–3311.
22 Willmann D, Lim S, Wetzel S, *et al*. Impairment of prostate cancer cell growth by a selective and reversible lysine-specific demethylase 1 inhibitor. *Int J Cancer* 2012; **131**: 2704–2709.
23 Vasilatos SN, Katz TA, Oesterreich S, Wan Y, Davidson NE, Huang Y. Crosstalk between lysine-specific demethylase 1 (LSD1) and histone deacetylases mediates antineoplastic efficacy of HDAC inhibitors in human breast cancer cells. *Carcinogenesis* 2013; **34**: 1196–1207.
24 Abdulla A, Zhao X, Yang F. Natural polyphenols inhibit lysine-specific demethylase-1 *in vitro*. *J Biochem Pharmacol Res* 2013; **1**: 56–63.
25 Sakane C, Okitsu T, Wada A, Sagami H, Shidoji Y. Inhibition of lysine-specific demethylase 1 by the acyclic diterpenoid geranylgeranoic acid and its derivatives. *Biochem Biophys Res Commun* 2014; **444**: 24–29.